

Effect of Alkali Hydroxides on the Strength and Fatigue of Fused Silica Optical Fiber

M. John Matthewson,* Vincenzo V. Rondinella,* Bochien Lin,* and Scott W. Keyes*

Fiber Optic Materials Research Program, Department of Ceramic Science and Engineering, Rutgers University, Piscataway, New Jersey 08855-0909

A two-point bend technique is used to determine the strength of "pristine" bare fused silica optical fiber in aqueous solutions of the group I alkali metal hydroxides (Li through Cs) in the concentration range $10^{-4}N$ to $1N$ (pH range 10 to 14). In the highest concentration solutions, a strong cation effect is exhibited with a minimum strength for KOH while fibers in LiOH and CsOH are typically 20% and 10% stronger, respectively. The cation effect decreases with decreasing concentration until at $10^{-4}N$ no effect is apparent. Tetramethylammonium hydroxide gives intermediate strengths between CsOH and LiOH. The results correlate closely with published results for the dissolution rate of silica which exhibit a maximum rate for KOH. In contrast, the results do not correlate with published subcritical crack growth data which show no cation effect for Na through Cs. These results support the pit etching model for pristine fiber strength proposed by Kurkjian *et al.* and argue against the presence of cracks or cracklike objects in these materials. [Key words: optical fibers, strength, fatigue, alkalies, hydroxides.]

I. Introduction

CERAMIC materials in general, and oxide glasses in particular, exhibit delayed failure; i.e., failure can occur after prolonged application of a constant stress which is significantly lower than the stress required to produce catastrophic failure. This phenomenon has important implications on the long-term reliability of ceramic components. Delayed failure is well understood for most ceramic materials and is due to the slow growth of preexisting cracks brought about by stress-enhanced environmental attack of the strained bonds at the crack tip. Wiederhorn¹ determined that a power law may be used to describe the empirical relationship between the rate of growth of a macroscopic crack, V , and the applied stress intensity factor, K_I :

$$V = AK_I^n \quad (1)$$

When combined with the well-known Griffith relation,

$$K_I = \sigma Yc^{1/2} \quad (2)$$

Eq. (1) may be integrated to predict the relationship between the time to failure, t_f , and the applied stress, σ_a , (static fatigue).¹

$$t_f = 2\sigma_a^{-n} \frac{1}{AY^2(n-2)} \left(\frac{\sigma_i}{K_{IC}} \right)^{n-2} \quad (3)$$

T. A. Michalske—contributing editor

Manuscript No. 197496. Received June 20, 1990; approved June 27, 1991. Supported in part by a grant from the New Jersey State Commission on Science and Technology and in part by the Fiber Optic Materials Research Program at Rutgers University.

*Member, American Ceramic Society.

or the relationship between strength, σ , and the loading rate, $d\sigma/dt$, (dynamic fatigue),¹

$$\sigma^{n+1} = 2 \frac{d\sigma}{dt} \frac{(n+1)}{(n-2)} \left(\frac{\sigma_i}{K_{IC}} \right)^{n-2} \frac{1}{AY^2} \quad (4)$$

where σ_i is the inert strength.

Michalske and Freiman² proposed a molecular mechanism for crack growth in fused silica in which water molecules directly attack the strained $-\text{Si}-\text{O}-\text{Si}-$ bonds at the crack tip to produce two silanol groups, $-\text{Si}-\text{OH}$ and $\text{HO}-\text{Si}-$. White, Freiman, Wiederhorn and Coyle³ found that the crack growth rate in silica increases with increasing pH and suggested that a second mechanism by which the silicon is attacked by a hydroxide ion enhances crack growth at high pH.

The fatigue characteristics of high-strength "pristine" silica optical fiber are qualitatively similar but there are significant quantitative differences. Kurkjian, Krause, and Paek⁴ suggested that, since the strength of silica fibers at liquid nitrogen temperatures is close to the theoretical ultimate strength of silica and since the distribution of strengths is very narrow and essentially single valued, the fibers are practically flaw-free and do not contain sharp, well-defined cracks. Therefore, the application of the crack growth theory described above to this material is inappropriate. However, a power law relationship between applied stress and time to failure has been observed for static fatigue of fiber, as is predicted by the crack growth model based on a power law $V-K_I$ relationship (Eq. (3)). This has led many workers to use the crack growth theory to make lifetime predictions for fibers despite the fact that the accepted value for the stress corrosion susceptibility parameter, n , determined from fiber static or dynamic fatigue is generally around 20, while the value for crack-containing bulk silica is around 40 from both direct crack growth measurements⁵ and static and dynamic fatigue experiments.^{6,7} In addition, it is now well established by workers from several laboratories that, at least in a liquid aqueous environment, the simple power law fatigue breaks down for bare and most polymer-coated fibers at sufficiently low applied stress/long time to failure, and "enhanced" fatigue is observed with a lower value of n , typically around 10.⁸⁻¹¹ This behavior cannot be explained by crack growth kinetics if some smooth growth law function is assumed instead of Eq. (1), because of the abruptness of the fatigue "knee."

The results we present here for silica fiber strength in various hydroxide solutions show a further difference between the fiber behavior and that expected from crack growth considerations. However, the results are somewhat more positive as they suggest possible mechanisms for fiber fatigue.

Since the fiber does not contain sharp cracks, yet does eventually fail by fast crack propagation, the fatigue mechanism must involve crack initiation as the rate-controlling step. Two initiation processes have been proposed in the literature. Kurkjian *et al.*⁴ noted that silica fibers aged under zero stress have a reduced strength which is comparable to that of initially weak silica rods strengthened by etching or aging. This observation may be explained if the two cases result in sur-

face features that are similar in shape but not size. The fiber fatigue is then controlled by the formation and subsequent growth of surface "pits" that arise from differential corrosion rates brought about by both fluctuations in the glass structure and differences in local stress as the pit develops.

Dabbs and Lawn¹² found that the stress corrosion parameter, n , for fibers weakened by a "subthreshold" Vickers indentation (i.e., an indentation performed at sufficiently low load to avoid radial crack formation) is similar to that for pristine fiber (~ 20). They therefore suggest that the crack initiation stage in high-strength silica is controlled by residual stresses around defects, such as handling damage or foreign particles that became attached to the fiber during the drawing process. While this might well be a reasonable model for weak fiber it is hard to envisage such regions of residual stress in the highest-strength fibers. In addition, Matthewson and Kurkjian¹³ pointed out that since the fatigue behavior in tension and two-point bending is similar and since the effective tested length in bending is only a few tens of micrometers, an unreasonably high density of subthreshold indentation-like defects would be needed. However, while the pit model does not provide, as yet, a detailed account of the mechanisms involved, it does appear the more reasonable for pristine fiber.

A survey of the literature shows that, qualitatively at least, the fatigue of silica fiber is sensitive to the same parameters as the fatigue of bulk crack-containing silica in a way consistent with strained bonds being ruptured by water or hydroxyl attack. Strength or time to failure decrease with increasing temperature and humidity (e.g., Duncan, France, and Craig¹⁴) and increasing pH (e.g., Matthewson and Kurkjian¹³), reflecting the link between decreasing strength and increasing water and hydroxyl activity and availability. The influence of different ionic species in the environment (other than hydroxide) has been largely ignored, probably because under most conditions the influence is small (although recent work shows a strength dependence on sodium chloride concentrations as well as on some other simple salts^{15,16}). This paper presents results for strength and dynamic fatigue measurements in various hydroxides, and it is found that at high pH the nature of the cations does significantly influence the strength.

II. Experimental Procedure

The strength of optical fiber has been measured using the two-point bend apparatus shown schematically in Fig. 1. First described by Murgatroyd,¹⁷ the technique involves bending the fiber between two grooved face plates which are then brought together until the fiber breaks. Figure 1 shows the modified version of the apparatus¹⁸ in which the fiber is not held between the plates by grooves but is loosely clamped to

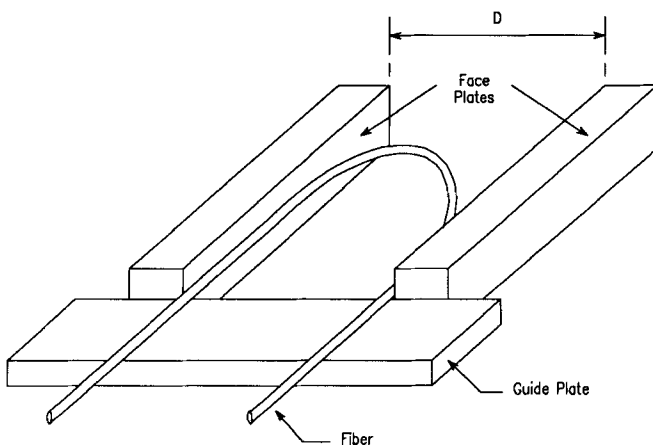


Fig. 1. Schematic of the two-point bend apparatus for determining fiber strength.

the guide plate. The flat polished face plates then do not damage the fiber surface, so that unprotected bare fiber can be used as well as polymer-coated fiber. The two-point bend technique is particularly simple to use, since there are no gripping problems and the fiber and face plates can easily be immersed in an environment.¹⁸ The face plates are brought together by a computer-controlled stepper motor until the fiber breaks. An acoustic transducer and trigger circuit detect the break and halt the stepper motor. The maximum strain on the fiber is at the tip of the bend and is calculated from the face plate separation at failure, D , using

$$\epsilon_f = 2.396 \frac{r}{D - d} \quad (5)$$

where r is the fiber radius and d is the overall fiber diameter, including any coating material. All strength results presented here will be in terms of the strain to failure, ϵ_f , since the two-point bend technique essentially measures strain, not stress. This avoids converting to stress via the elastic modulus, which is nonlinear at the strains encountered in these experiments (e.g., Krause, Testardi and Thurston¹⁹).

The fiber used in this study was 125- μm diameter silica coated with a UV-curable polyurethane acrylate. Since this work is concerned with the interactions of the silica with the environment, the polymer coating was stripped from the test section of the fiber using hot concentrated sulfuric acid so that in Eq. (5) $2r = d = 125 \mu\text{m}$. While bare fiber behavior is of academic interest—with the current poor understanding of the details of fiber fatigue it is hardly likely that coated fiber fatigue can be understood when the coating at the very least confuses the situation by acting as a diffusion barrier—the results of Matthewson and Kurkjian¹³ imply that results for bare fiber under accelerated testing conditions are a better model for polymer-coated fiber under long-term in-service conditions because the rate-controlling step for fatigue in both cases is corrosion of the silica surface. For coated fiber under accelerated conditions, testing times may be comparable with diffusion times through the coating, making interpretation of the results difficult.

Solutions of LiOH, NaOH, KOH, RbOH, CsOH, and tetramethylammonium hydroxide (TMA, $(\text{CH}_3)_4\text{NOH}$) were prepared in concentrations of 1N, 0.01N, and 10^{-4} N in deionized water using the gravimetric data supplied by the manufacturers of the starting compounds. Care was taken to keep all materials tightly stoppered to minimize adsorption of atmospheric water and carbon dioxide. For simplicity, testing was carried out in these solutions at ambient laboratory temperature, which was measured when each specimen was tested. The temperatures fluctuated by typically $\pm 2^\circ\text{C}$ around a mean of 22°C , although for a few days the mean temperature rose to 27°C , which had a noticeable effect on the strength. The temperature dependence of strength was measured in 0.01N KOH in the temperature range 0° to 60°C at a constant face plate velocity of $100 \mu\text{m} \cdot \text{s}^{-1}$. An Arrhenius plot of the results is shown in Fig. 2. The data fit a straight line well, whose slope gives an effective activation energy of $E_{\text{eff}} = (1.85 \pm 0.19) \text{ kJ} \cdot \text{mol}^{-1}$ (all confidence limits quoted in this paper, both explicitly and graphically, represent a 95% interval). This is not a true activation energy, since the reciprocal of the strain to failure is not a direct measure of the rate of a thermally activated process. France, Paradine, and Beales,²⁰ following the crack growth analysis of Wiederhorn,¹ showed that the dynamic fatigue equation in two-point bend under conditions of constant face plate velocity, v , becomes

$$\epsilon_f^{n-1} = \frac{(n-1)}{(n-2)} \left(\frac{\sigma_i}{K_{\text{IC}}} \right)^{n-2} \frac{0.82v}{rAY^2} \quad (6)$$

Since the assumed Arrhenius temperature dependence of the crack growth rate is in the rate constant A , then, assuming the activation energy is stress independent, the strain to failure is

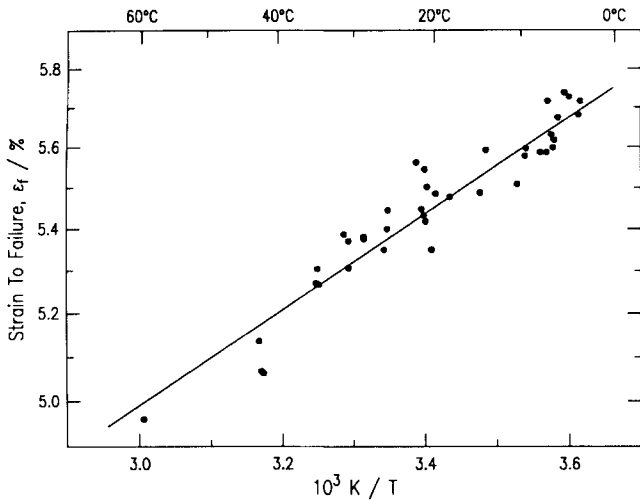


Fig. 2. Arrhenius plot of $\ln(\text{strain to failure})$ versus $1/T$ for the strength of bare fiber in 0.01N KOH. Face plate velocity $100 \mu\text{m} \cdot \text{s}^{-1}$.

of the form

$$\epsilon_f^{n-1} \sim v_c e^{E/RT} \quad (7)$$

so that

$$E = (n - 1)E_{\text{eff}} \quad (8)$$

The activation energy is determined to be $\sim 30 \text{ kJ} \cdot \text{mol}^{-1}$ from Fig. 2 if a value of $n \sim 16$ is assumed (q.v. below). This value is similar to but somewhat lower than published values. However, the value is not unreasonable, given that there is evidence that the activation energy is sensitive to both temperature¹⁴ and stress.^{22,*}

While this determination of activation energy assumes crack growth kinetics and one purpose of this paper is to emphasize the inapplicability of such a treatment to high-strength fibers, the estimated value is not inconsistent with published data. Further, n values deduced from dynamic fatigue experiments in two-point bending under conditions of constant stress rate (standard log-log fatigue plot slope $1/(n + 1)$, Eq. (4)) and constant face plate velocity (slope $1/(n - 1)$, Eq. (6)) are indistinguishable, while the slopes of the plots are distinguishable.²¹ This indicates that the forms of the crack growth equations are not entirely useless if used with caution as empirical scaling rules. However, n must then be redefined in terms of the slope of fatigue data plots and should not be thought of as an exponent in a crack growth rate equation.

All results presented here have been corrected for temperature variation and are calculated for a test temperature of 22°C (295 K). For simplicity a linear temperature dependence is used, since the temperature span is small:

$$\epsilon_f(295) = \epsilon_f(T)[1 + \alpha(T - 295)] \quad (9)$$

where α , calculated by replottting the data of Fig. 2 on linear axes, is found to be 0.0136 K^{-1} . It is assumed that, since the correction generally has a small effect on the mean strength, this value is appropriate for other alkalis and concentrations. The correction, however, does significantly reduce the scatter in the results.

*The observed stress dependence of the activation energy is an inconsistency with the power law (Eq. (1)), since stress then must also appear in the prefactor. *A*. Other models based on chemical kinetics account for the stress by its effect on the activation energy and result in exponential forms for Eq. (1). These different models generally fit fatigue data equally well, but they can profoundly affect lifetime predictions made by extrapolation.²³

Immediately after stripping the polymer coating in hot acid and washing, the fibers were loaded in the two-point bend apparatus at a face plate separation of 12 mm (1.3% strain) and immersed in the test solution for typically 10 min. For the slowest face plate velocity used ($1 \mu\text{m} \cdot \text{s}^{-1}$), the fibers were then loaded at high speed to no more than a half of the final breaking strain before continuing at the test velocity. This decreases the experimental duration without significantly perturbing the measured strength.

III. Results

Figure 3 shows the results for strength measurement of the bare fiber in 1N alkali at four different face plate velocities (note that the alkali metal hydroxides are plotted in order of increasing atomic number). Each point represents an average of 10 specimens; error bars represent a 95% confidence limit for the mean value. A pronounced cation effect is observed for the alkali metal hydroxides with a minimum strength for potassium. The strength in potassium represents a 20% reduction over that in lithium and a 10% to 15% reduction over that in cesium. The TMA strength is intermediate between those for cesium and lithium.

Figure 4 shows the data of Fig. 3 replotted as strain to failure as a function of face plate velocity on logarithmic axes. The data closely fit a power law dependence. Apart from the LiOH, the lines appear to converge, at least on these logarithmic scales, at a face plate velocity of the order of $0.1 \text{ m} \cdot \text{s}^{-1}$, corresponding to a time scale of a few microseconds. The stress corrosion parameter, n , may be determined from the slopes of these lines (Eq. (6)) and the results are shown in Fig. 5. While there may be some systematic trend with cation it is not statistically significant.

The measured values of n are somewhat lower than the generally accepted value of around 20 measured under more neutral conditions (pH ~ 7). However the results are consistent with static fatigue measurements at 90°C on stripped silica fiber by Krause and Shute,²⁴ who observed n fall from 21 at pH 7 to 13 at pH 14 (1N KOH). Dynamic fatigue data for 1N and 0.1N KOH indicate that the value of n increases from 14.4 ± 0.4 to 17.3 ± 0.5 as the pH decreases from 14 to 13 and is consistent with the published static fatigue data.

The results of Fig. 2 were obtained by breaking the fibers after immersion in the test environment for approximately 10 min at a low strain to allow equilibration. It is known that aging both multicomponent²⁵ and silica¹³ glass fiber under zero stress for prolonged periods of time results in strength loss. However, degradation is significant only at longer times

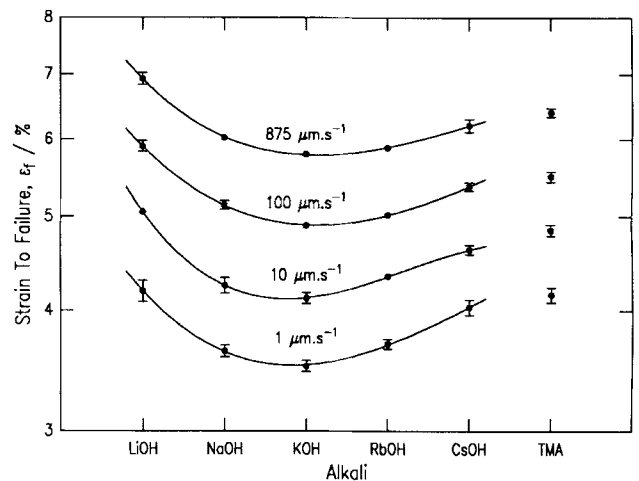


Fig. 3. Strain to failure as a function of 1N alkali for four different face plate velocities.

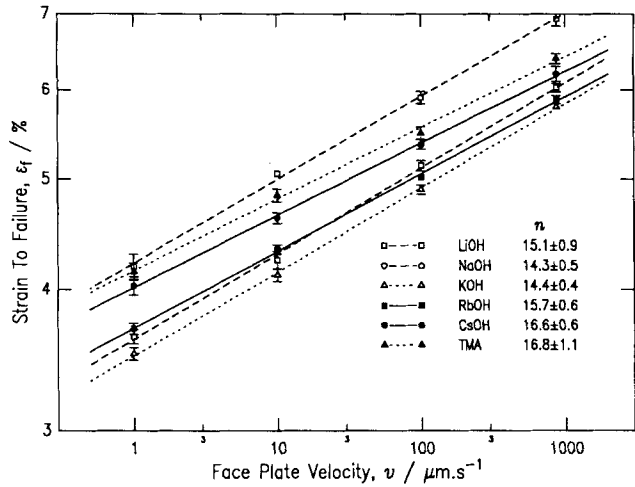


Fig. 4. Data of Fig. 3 replotted as dynamic fatigue curves.

and higher temperatures than used in this work.[†] To firmly establish that the equilibration time is not a key parameter, the fiber strength was measured in 1N KOH and CsOH at a face plate velocity of 100 μm·s⁻¹ for a range of pretest immersion times. The results, shown in Fig. 6, show no significant dependence on immersion time for a 3½ orders of magnitude span in time. This confirms that the variation in strength between the different alkali environments is a result of different corrosion rates during testing and is not caused by differential aging rates prior to testing. While zero stress aging is not an important effect in this work, we do not wish to minimize its importance when considering long-term reliability of optical fiber systems.

Figure 7 presents results for strength measurements of bare fiber as a function of alkali for three different ionic strengths and at a constant face plate velocity of 100 μm·s⁻¹. The cation effect observed in 1N solution is identical though less pronounced in 0.01N (nominal pH 12) solution, but the effect is not detectable at 10⁻⁴N (nominal pH 10). The cation effect is therefore important only in the most basic solutions, and this observation probably explains why ionic effects are not

[†]Krause²⁶ did observe strength degradation of bare silica fiber at room temperature on the time scale of a day, but more recent work on coated fiber (Krause, private communication) does not confirm the earlier results and attributes the degradation of the bare fiber to possible damage by impact with particulate contaminants in the test environment.

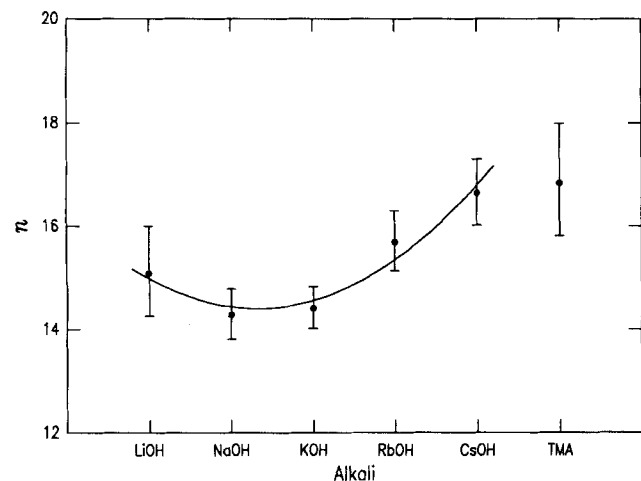


Fig. 5. Stress corrosion parameter, *n*, as a function of alkali for dynamic fatigue in 1N solution.

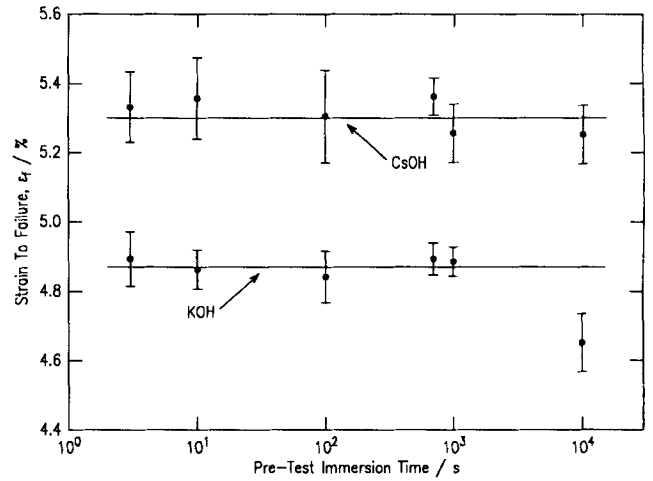


Fig. 6. Strength as a function of pretest immersion time in 1N KOH and CsOH for a face plate velocity of 100 μm·s⁻¹.

widely reported in the literature. Most optical fiber applications are concerned with more neutral environments (pH ~7), and investigations of ionic effects have been inconclusive. However, ionic effects can have practical relevance as well as academic, since fiber cables unintentionally immersed in household cleaners, for example, can experience a highly basic environment.

The experimental procedures used in this work were carefully designed to eliminate extraneous influences that might perturb the results so that differences between the cations, which were expected to be small, could be readily detected. In particular, strength measurements in different cations were interleaved (i.e., one fiber was broken in LiOH, another in NaOH, KOH, RbOH, CsOH, and TMA; this pattern was then repeated until 10 measurements had been taken in each solution) in order to eliminate systematic differences between the cations due to fluctuations in temperature or age of the test solutions. Aging of the solutions is particularly important, since they absorb atmospheric CO₂ and become partially neutralized. However, the experimental procedure does not preclude the possibility that the different solutions age at different rates. If, for example, KOH absorbed atmospheric carbon dioxide more slowly than did the other solutions, then its pH would be higher, leading to a lower strength. The apparent cation effect would then be readily explainable by the pH sensitivity of strength. Examination of Fig. 7 shows that fiber in 0.01N KOH is still weaker than fiber in 1N LiOH

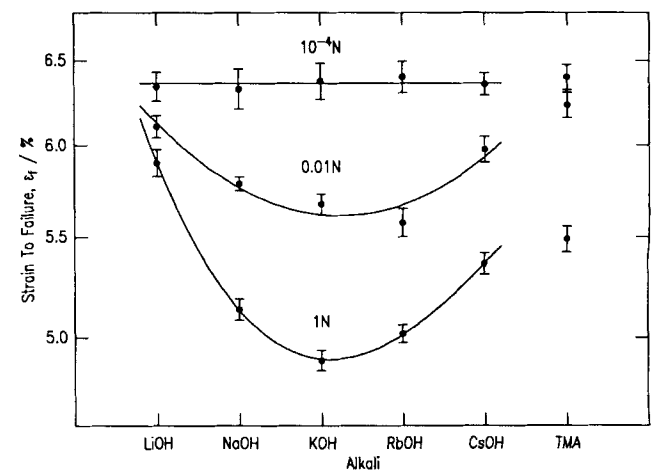


Fig. 7. Strength as a function of hydroxide for four different concentrations and a face plate velocity of 100 μm·s⁻¹.

despite a hundredfold decrease in (at least nominally) OH^- availability. Additionally, no correlation is observed between strength and the age of the solution; linear regression fits to the strength of individual fibers versus the solution age yield straight lines with a slope less than the standard error in the slope. This is true even for data taken at a face plate velocity of $1 \mu\text{m} \cdot \text{s}^{-1}$ for which the total experiment duration, and hence solution age at the end, was approximately one month.

A commercial pH meter was used to measure the pH of the solutions. Table I summarizes the results for the 1N solutions and compares unused solution kept in tightly closed bottles with the solutions used for the data of Fig. 2 taken at a jaw speed of $1 \mu\text{m} \cdot \text{s}^{-1}$. The latter solutions had been exposed to air for approximately 20 d. It should be noted that pH electrodes can show nonlinear response at high pH and that the nonlinearity depends to some extent on the nature of alkali metal cations present. This, coupled with the difficulty in calibrating the probe at high pH, explains why the nominal pH of 14 is not achieved. With the exception of LiOH, the pH values are very similar and, again with the exception of LiOH, are typically degraded ~ 0.2 pH by prolonged exposure to atmospheric CO_2 . LiOH does strongly absorb CO_2 to form Li_2CO_3 , which is only weakly soluble (white solid particles were observed on the surface of older LiOH solutions).

Lithium ions are known to strongly associate with hydroxide ions, thus reducing the hydroxide ion activity. Sodium ions also weakly associate with hydroxide ions. This behavior is reflected in the lower pH of these solutions, as indicated in Table I. It is therefore possible that the strength is higher in LiOH and NaOH than in KOH simply because of pH differences. Figure 8 shows the strength measured at a constant face plate velocity of $100 \mu\text{m} \cdot \text{s}^{-1}$ in various concentrations of KOH plotted as a function of the solution pH. Two values for the pH are used, firstly the nominal pH (1N gives a nominal pH of 14) and secondly the measured pH using a pH probe calibrated in pH 7 and 10 buffers. The data fit straight lines quite well so that strains to failure, ϵ_1 and ϵ_2 , measured in pH's pH_1 and pH_2 , can be related by

$$\epsilon_1 = \epsilon_2 m^{(\text{pH}_2 - \text{pH}_1)} \quad (10)$$

where m , derived from the slopes, has values of 1.070 for the nominal pH and 1.056 for the measured pH. Figure 9 shows the as-measured strain to failure data from Fig. 3 for a face plate velocity of $100 \mu\text{m} \cdot \text{s}^{-1}$ and compares them to the same data with the LiOH and NaOH strengths corrected from their measured pH to the measured pH for KOH (Table I) using Eq. (10) and a value of $m = 1.056$. The minimum strength for KOH is still apparent, so that pH effects alone cannot explain the observed behavior.

All the above arguments indicate that the cation effect is actually due to the presence of different cationic species and is not (except perhaps partially for lithium) due to different effective hydroxide concentrations. The alkali metal ions therefore appear to play a direct role in the chemical reactions and have different powers of promoting the strength degradation. Such behavior suggests the cations have a catalytic action.

IV. Discussion

The data presented here are the first showing such a cation effect on strength and fatigue of pristine optical fibers. White, Freiman, Wiederhorn, and Coyle³ investigated macroscopic crack growth velocities in silica glass for similar environments. They found that the crack growth velocities in 1N

Table I. Indicated pH of 1N Solutions

	LiOH	NaOH	KOH	RbOH	CsOH	TMA
Unused	12.25	12.85	13.15	13.24		
Used	11.75	12.65	12.95	13.12	13.12	13.16

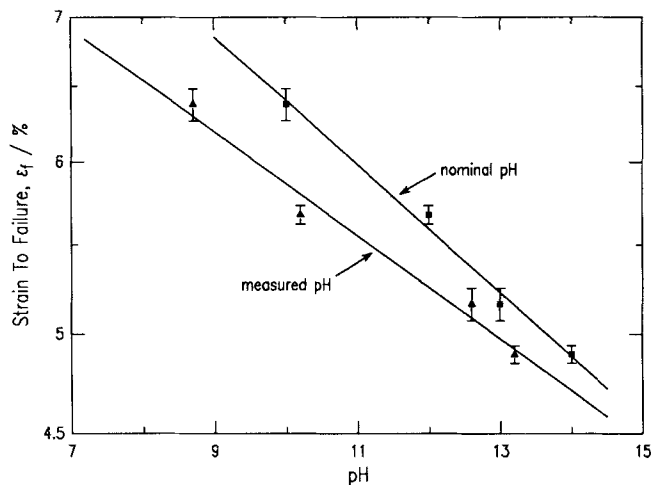


Fig. 8. Strength as a function of pH (both nominal and as measured) for various concentrations of KOH and a face plate velocity of $100 \mu\text{m} \cdot \text{s}^{-1}$.

NaOH, KOH, and CsOH were very similar, while that in LiOH was slower and similar to velocity measurements made in water. No cation effect was observed in 0.001N solutions. They attributed the anomalous lithium results at 1N concentrations to the strong lithium/hydroxide association, partially due to simple reduction of hydroxide activity in the bulk liquid but also partially due to lithium trapping hydroxide ions in the confines of the crack. While these results have similarities to those presented here, namely the difference between cations is only observed at high pH and lithium gives the slowest corrosion rate in both cases, detailed correlation is poor but not unexpected, given the absence of well-defined cracks in the pristine fiber material.⁴

Ionic effects are well-known in the sol-gel chemistry field, and in particular the dissolution of silica is known to be cation dependent. In recent work, Wijnen, Beelen, de Haan, Rummens, van de Ven and van Santen²⁷ used ^{29}Si -NMR to examine the dissolution rate of pyrogenic silica (submicrometer silica particles with essentially the same internal structure as bulk fused silica) in 1N and 3N alkali metal hydroxides (actually 2:3:108 and 2:1:35 molar mixtures of MOH, SiO_2 , and H_2O). Figure 10 shows these results for the dissolution rate in 3N solution. The dissolution rate shows a marked peak at potassium and exhibits remarkable correlation with the strength results of Fig. 2; the solutions giving the lowest strength exhibit the highest dissolution rates. The dissolution rates in 1N solution were found to show similar effects,

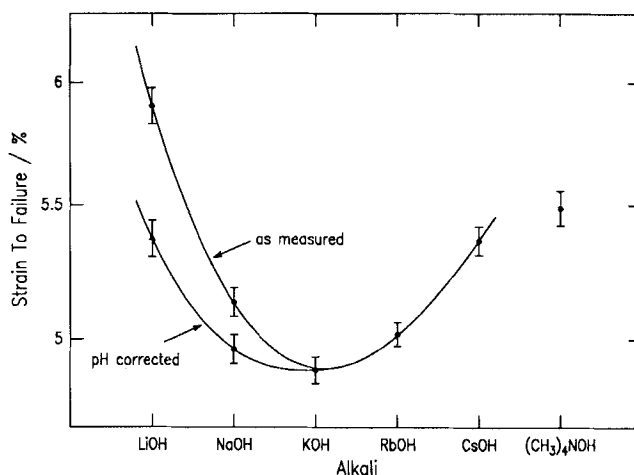


Fig. 9. As-measured and pH-corrected strength as a function of alkali hydroxide for a face plate velocity of $100 \mu\text{m} \cdot \text{s}^{-1}$.

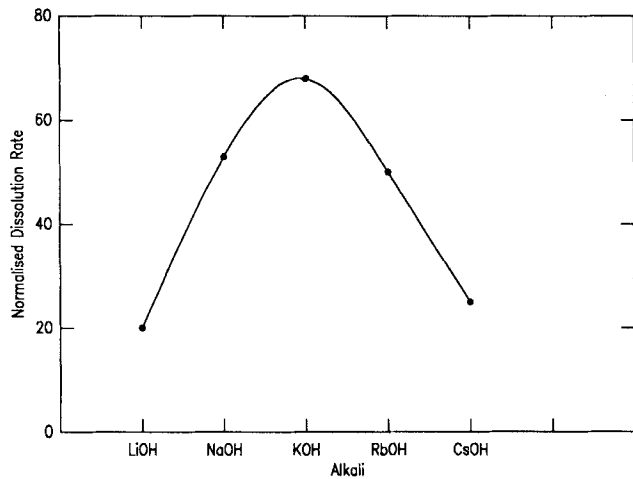


Fig. 10. Rate of dissolution of silica in various 3N alkalis (from Wijnen *et al.*²⁷)

though the differences between the cations were less pronounced. The reasons for this behavior are complex and not well understood but are concerned with the way the cations associate to different extents with both the silica surface and the various silica oligomers formed after dissolution. Additionally, the transport of the negative hydroxide ions to the negative silica surface is thought to be mediated by the cations. The "catalytic" strength of the different cations depends on the both the binding energy and size of the cation's hydration shell.

The strong correlation between dissolution rate and strength suggests that the strength-degrading mechanism might involve dissolution; it does not constitute proof, though, especially since many aspects of silica chemistry are cation dependent. However, such a correlation would be expected from the "pit" model of Kurkjian *et al.*⁴ In this model, the "perfect" silica surface is etched at different rates because of structure fluctuations in the material. The surface pits so formed act as stress concentrators, and stress-assisted etching takes place. The differential etching rates around the pit cause it, in contrast to the crack growth model, to change shape as well as depth. If the etching process is simply dissolution, then the results presented here are to be expected from the published dissolution rate data. The correlation with dissolution data and the observation that the different ions are distinguishable on submillisecond time scales, coupled with the insensitivity of strength to the presoak time, suggest that the early rate-controlling stages of high-strength fiber fatigue is an essentially free-surface or near-surface process and does not involve diffusion of reactants into and products out of the body of the silica.

The interpretation of the pit model in terms of dissolution is described, at least qualitatively, by the flaw growth model of Hillig and Charles²⁸ in which the flaw tip geometry changes because of a stress-dependent corrosion reaction. However, the results of analyzing this model are not directly applicable to high-strength fiber, firstly because the model assumes the flaw is very much longer than it is wide. Secondly, the continuum nature of the model is not appropriate to the molecular length scale envisaged for the pit model when the discrete nature of the pit etching is expected to have a strong influence.²⁹

Direct evidence of pit etching has recently been obtained using both scanning tunneling³⁰ and atomic force microscopy³¹ on the surface of fibers aged for up to several months in 85°C water. This work shows that surface roughness develops whose amplitude correlates with the residual strength of the fiber after aging. While this work is not directly applicable to our results, since the experiment duration is much longer and the surface features are much larger than expected here, it does

prove the existence of etching processes and illustrates their importance.

The difference in behavior between crack growth kinetics and pristine fiber strength implies that there is, at some intermediate strength, a transition between the two types of cation dependence. Recent work in our laboratory has used "subthreshold" Vickers indentations on fibers to model weaker material,¹² and preliminary results indicate that there is an abrupt transition with fibers indented by a 10-mN load (1% strain to failure in 1N KOH), showing behavior identical to the pristine fiber with a well-defined minimum strength in KOH, while behavior identical to the crack growth results, with no cation dependence except for LiOH, is observed for 100-mN indentations (0.6% strain to failure).³² The cation dependence observed here is therefore relevant only to the strongest fibers, though this strength range does encompass typical proof test stresses for optical fibers and is therefore of great practical interest.

V. Conclusions

Results are presented for the strength and dynamic fatigue of bare silica optical fiber in aqueous alkali metal hydroxides and tetramethylammonium at various concentrations. In 1N solution a strong cation effect is observed, with KOH giving the lowest strength. The effect diminishes in more dilute solutions and is not apparent at 10⁻⁴N. These results do not correlate with published crack growth rate measurements and imply that, at least at high pH, the subcritical crack growth model is not appropriate for describing the fatigue behavior of high-strength silica optical fiber. In contrast, the cation effect correlates closely with published dissolution rate data, with a maximum rate for KOH corresponding to the minimum strength. This suggests that the early stages of fatigue are controlled by etching the pristine surface, therefore implying that the rate-controlling stage of fiber fatigue is probably a free surface phenomenon.

These results for bare fibers, while shedding light on fatigue mechanisms, also have practical relevance to the reliability of polymer-coated optical fiber. Under conditions of low applied stress and long times to failure, the coating is not expected to act as an important diffusion barrier. Thus the short-term experiments on bare fiber are a better model for long-term reliability than short-term experiments on coated fiber when the coating will act as a significant diffusion barrier to reactants and reaction products. Optical fiber cables can experience very high hydroxide concentrations in some applications when, for example, the cable is exposed to highly basic cleaners.

References

- S. M. Wiederhorn, "Subcritical Crack Growth in Ceramics"; pp. 613-46 in *Fracture Mechanics of Ceramics*, Vol. 2. Edited by R. C. Bradt, D. P. H. Hasselman, and F. F. Lange. Plenum Press, New York, 1974.
- T. A. Michalske and S. W. Freiman, "A Molecular Mechanism for Stress Corrosion in Vitreous Silica," *J. Am. Ceram. Soc.*, **66** [4] 284-88 (1983).
- G. S. White, S. W. Freiman, S. M. Wiederhorn, and T. D. Coyle, "Effects of Counterions on Crack Growth in Vitreous Silica," *J. Am. Ceram. Soc.*, **70** [12] 891-95 (1987).
- C. R. Kurkjian, J. T. Krause, and U. C. Paek, "Tensile Strength Characteristics of "Perfect" Silica Fibers," *J. Phys. C: Solid State Phys.*, **43** [12] C9-585-586 (1982).
- S. Sakaguchi, Y. Hibino, and Y. Tajima, "Fatigue in Silica Glass for Optical Fibers," *Rev. Electr. Commun. Lab.*, **32** [3] 444-51 (1984).
- S. Sakaguchi, Y. Sawaki, Y. Abe, and T. Kawasaki, "Delayed Failure in Silica Glass," *J. Mater. Sci.*, **17**, 2878-86 (1982).
- J. E. Ritter, Jr., and C. L. Sherburne, "Dynamic and Static Fatigue of Silicate Glasses," *J. Am. Ceram. Soc.*, **54** [12] 601-605 (1971).
- J. T. Krause, "Transitions in the Static Fatigue of Fused Silica Fiber Lightguides"; pp. 19.11-19.14 in *Proceedings of the 5th European Conference on Optic Communications* (Amsterdam, Netherlands, 1979), post deadline paper.
- H. C. Chandan and D. Kalish, "Temperature Dependence of Static Fatigue of Optical Fibers Coated with a UV-Curable Polyurethane Acrylate," *J. Am. Ceram. Soc.*, **65** [3] 171-73 (1988).

- ¹⁰M. J. Matthewson, C. R. Kurkjian, and J. T. Krause, "Static Fatigue Testing of Optical Fibers," *Am. Ceram. Soc. Bull.*, **64** [3] 468 (1985).
- ¹¹D. Roberts, E. Cuellar, and L. Middleman, "Static Fatigue of Optical Fibers in Bending II: Effect of Humidity and Proof Stress on Fatigue Lifetimes"; in Proceedings of SPIE Symposium on Fiber Optics and Integrated Optoelectronics (San Diego, CA, Aug. 16–21, 1987).
- ¹²T. P. Dabbs and B. R. Lawn, "Strength and Fatigue Properties of Optical Glass Fibers Containing Microindentation Flaws," *J. Am. Ceram. Soc.*, **68** [11] 563–69 (1985).
- ¹³M. J. Matthewson and C. R. Kurkjian, "Environmental Effects on the Static Fatigue of Silica Optical Fiber," *J. Am. Ceram. Soc.*, **71** [3] 177–83 (1988).
- ¹⁴W. J. Duncan, P. W. France, and S. P. Craig, "The Effect of Environment on the Strength of Optical Fiber"; pp. 309–28 in "The Strength of Glass." Edited by C. R. Kurkjian. Plenum Press, New York, 1985.
- ¹⁵D. Inniss, D. L. Brownlow, and C. R. Kurkjian, "Effect of Salts on the Static Fatigue of Silica Optical Fibers"; presented at the 92d Annual Meeting of the American Ceramic Society, Dallas, TX, April 23, 1990 (Ceramic Matrix Composites Symposium, Paper No. 9-SIV -90).
- ¹⁶V. V. Rondinella and M. J. Matthewson, "Influence of Solutes on the Fatigue Behavior of Pristine Silica Optical Fiber," *Ceram. Trans.*, in press.
- ¹⁷J. B. Murgatroyd, "The Strength of Glass Fibers. Part II. The Effect of Heat Treatment on Strength," *J. Soc. Glass Technol.*, **28**, 388–405 (1944).
- ¹⁸M. J. Matthewson, C. R. Kurkjian, and S. T. Gulati, "Strength Measurement of Optical Fibers by Bending," *J. Am. Ceram. Soc.*, **69** [11] 815–21 (1986).
- ¹⁹J. T. Krause, L. R. Testardi, and R. N. Thurston, "Deviations from Linearity in the Dependence of Elongation upon Force for Fibers of Simple Glass Formers and of Glass Optical Lightguides," *Phys. Chem. Glasses*, **20** [6] 135–39 (1979).
- ²⁰P. W. France, M. J. Paradine, and K. J. Beales, "Ultimate Strength of Glasses Used for Optical Communications"; in Proceedings of the 12th International Congress on Glass (Albuquerque, NM). North-Holland, Amsterdam, Netherlands, 1980.
- ²¹V. V. Rondinella and M. J. Matthewson, "Effect of Loading Rate Scheme on the Dynamic Fatigue of Fused Silica Fiber"; unpublished work.
- ²²C. K. Kao, "Optical Fibre and Cables"; in *Optical Fibre Communications*. Edited by M. J. Howes and D. V. Morgan. Wiley, New York, 1980.
- ²³G. M. Bubel and M. J. Matthewson, "Optical Fiber Reliability Implications of Uncertainty in the Fatigue Crack Growth Model," *Opt. Eng.*, **30** [6] 737–45 (1991).
- ²⁴J. T. Krause and C. J. Shute, "Temperature Dependence of the Transition in Static Fatigue of Fused Silica Optical Fiber," *Adv. Ceram. Mater.*, **3** [2] 118–21 (1988).
- ²⁵P. W. France, W. J. Duncan, D. J. Smith, and K. J. Beales, "Strength and Fatigue of Multicomponent Optical Glass Fibres," *J. Mater. Sci.*, **18**, 785–92 (1983).
- ²⁶J. T. Krause, "Zero Stress Strength Reduction and Transitions in Static Fatigue of Fused Silica Fiber Lightguides," *J. Non-Cryst. Solids*, **38–39**, 497–502 (1980).
- ²⁷P. W. J. G. Wijnjen, T. P. M. Beelen, J. W. de Haan, C. P. J. Rummens, L. J. M. van de Ven, and R. A. van Santen, "Silica Gel Dissolution in Aqueous Alkali Metal Hydroxides Studied by ²⁹Si-NMR," *J. Non-Cryst. Solids*, **109**, 85–94 (1989).
- ²⁸W. B. Hillig and R. J. Charles, "Surfaces, Stress-Dependent Surface Reactions, and Strength"; pp. 682–705 in *High Strength Materials*. Edited by V. F. Jackey. Wiley, New York, 1965.
- ²⁹I. F. Scanlan, "Computer-Aided Bond Failure Model of Crack Growth in Silica"; presented at the 91st Annual Meeting of the American Ceramic Society, Indianapolis, IN, April 26, 1989 (Glass Division, Paper No. 71-G-89).
- ³⁰R. S. Robinson and H. H. Yuce, "Scanning Tunneling Microscopy Study of Optical Fiber Corrosion: Surface Roughness Contribution to Zero-Stress Aging," *J. Am. Ceram. Soc.*, **74** [4] 814–18 (1991).
- ³¹H. H. Yuce, J. P. Varachi, and P. L. Key, "Effect of Zero-Stress Aging on Mechanical Behavior of Optical Fibers," *Ceram. Trans.*, in press.
- ³²M. J. Matthewson, B. Lin, and V. V. Rondinella, "Effect of Solutes on the Fatigue Behavior of Silica Optical Fiber," *OFC Tech. Digest*, **4**, 158 (1991). □